Free-Standing Hybrid Anion-Exchange Membranes for Application in Fuel Cells

Xiaocheng Lin,[1] Cuiming Wu,[2] Yonghui Wu,[1] Tongwen Xu[1]

[1]*CAS Key Laboratory of Soft Matter Chemistry, Laboratory of Functional Membranes, School of Chemistry and Materials Science, University of Science and Technology of China, Hefei, Anhui 230026, People's Republic of China*
[2]*School of Chemical Engineering, Hefei University of Technology, Hefei, Anhui 230009, People's Republic of China*

ABSTRACT: A series of free-standing hybrid anion-exchange membranes were prepared by blending brominated poly(2,6-dimethyl-1,4-phenylene oxide) (BPPO) with poly(vinylbenzyl chloride-*co*-γ-methacryloxypropyl trimethoxy silane) (poly(VBC-*co*-γ-MPS)). Apart from a good compatibility between organic and inorganic phases, the hybrid membranes had a water uptake of 32.4–51.8%, tensile strength around 30 MPa, and T_d temperature at 5% weight loss around 243–261°C. As compared with the membrane prepared from poly (VBC-*co*-γ-MPS), the hybrid membranes exhibited much better flexibility, and larger ion-exchange capacity (2.19–2.27 mmol g^{-1}) and hydroxyl (OH^-) conductivity (0.0067–0.012 S cm^{-1}). In particular, the hybrid membranes with 60–75 wt % BPPO had the optimum water uptake, miscibility between components, and OH^- conductivity, and were promising for application in fuel cells. © 2011 Wiley Periodicals, Inc. J Appl Polym Sci 123: 3644–3651, 2012

Key words: anion-exchange membrane; hybrid membrane; fuel cell; sol–gel

INTRODUCTION

The solid polymer electrolyte membrane fuel cells, due to high power density and efficiency, have been developed for use as portable or mobile power sources.[1] As a critical component, the ion-exchange membrane is required to have high conductivity as well as chemical, thermal, and electrochemical stabilities.[1,2] Generally, fuel cell membranes are prepared from organic polymers, such as poly(vinylidene fluoride) (PVDF),[3–5] polysulfone (PS),[6,7] and poly(ether ether ketone) (PEEK).[8,9] However, these membranes have inherent drawbacks—high methanol crossover and swelling,[10–12] and thus need further improvements. In particular, incorporation of inorganic components into organic polymers (i.e., inorganic–organic hybridization) became a focus of attention.[13–17] As compared with the original organic polymers, the hybrid membranes may possess not only higher mechanical, thermal, and chemical stabilities[15] but also reduced methanol crossover and high conductivity.[16,17]

To date, proton-exchange hybrid membrane fuel cells (PEMFCs) have been widely investigated; unfortunately, the preparation of hybrid anion-exchange membranes for alkaline membrane fuel cells (AMFCs) is studied insufficiently. These AMFCs have such unique features as: low methanol crossover, high catalytic efficiency, diverse catalyst categories, more facile methanol oxidation and oxygen reduction, and easy water management.[2] Therefore, exploration in this direction is also of significance.

For preparation of hybrid anion-exchange membranes, sol–gel process is commonly performed. Alkoxysilanes, such as tetraethoxysilane (TEOS), can be mixed with anion-exchange polymers for *in situ* sol–gel reaction.[18,19] The inorganic component interacts with the organic polymers mainly through weak interactions, such as van der Waals attraction or hydrogen-bonding. To reinforce the interaction, one can modify polymers with functional groups, such as alkoxysilanes. In this way, the polymers can take part in the sol–gel process and form strong covalent bonds with the inorganic components. In our previous work, the latter route was used. Organic monomer and organically modified alkoxysilanes were copolymerized to form the "multi-alkoxy" polymer precursor.[20–22] This kind of precursor contains a
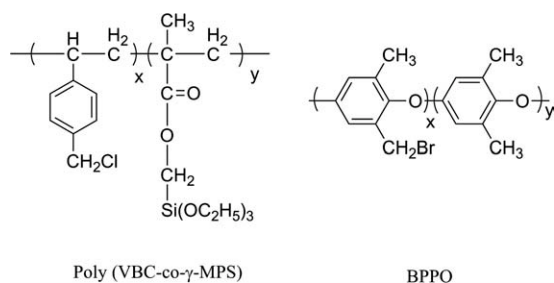
Scheme 1 Schematic of the structures of poly(VBC-*co*-γ-MPS) and BPPO.

plenty of pendant alkoxysilane groups, which can form strong silica networks after sol–gel with other alkoxysilanes, such as TEOS or monophenyltriethoxysilane (EPh). Several series of hybrid membranes were prepared by this means and exhibited good physicochemical properties.[21,22] Among these membranes, one series prepared from the copolymer of vinylbenzyl chloride (VBC) and γ-methacryloxypropyl trimethoxy silane (γ-MPS) (poly(VBC-*co*-γ-MPS)) were tested for use in AMFCs. Unfortunately, the conductivity was relatively low (2.27×10^{-4} to 4.33×10^{-4} S cm^{-1}). The main cause is the use of polyethylene terephthalate (PET) woven fibers as the supporting material, which makes the membrane low in hydrophilicity (water content, 16–35%).[22]

To explore a better membrane, this research focuses on the preparation of free-standing hybrid anion-exchange membranes by blending poly(VBC-*co*-γ-MPS) with brominated poly(2, 6-dimethyl-1,4-phenylene oxide) (BPPO). As a unique engineering plastic polymer, BPPO can be easily quaternized into highly anion-exchange and OH$^-$-conductive materials.[23] Besides, its mechanical properties, physicochemical and thermal stabilities are outstanding.[23,24] By blending BPPO with poly(VBC-*co*-γ-MPS), free-standing membranes without supporting materials may be obtained. On the other hand, poly(VBC-*co*-γ-MPS) and BPPO (as shown in Scheme 1) both have benzyl halogenide groups in the main chains, and thus good miscibility between them can be expected. The conditions of membrane preparation will be optimized for fuel cell applications.

EXPERIMENTAL

Materials

BPPO (M_w = 60,500) with a benzyle substitution ratio of 0.73 was provided by Tianwei Membrane Co. Ltd., Shandong, China and was dissolved in toluene to prepare a solution (0.23 g mL^{-1} BPPO). VBC, γ-MPS, toluene, dimethyl formamide (DMF), trimethylamine (TMA), ethanol, and KOH were all of analytical grade. DMF and toluene were kept in molecular sieve before use. TMA was collected from an aqueous solution (33%) by using DMF and a solution of 3.99 mol L^{-1} TMA was thus prepared. Azobisisobutyronitrile (AIBN) was purified before use by dissolving in methanol (35°C), recrystallization in an ice bath, and then drying in a vacuum oven at room temperature. Deionized water was used throughout. The other reagents were used as received.

Preparation of poly(VBC-*co*-γ-MPS)

Poly(VBC-*co*-γ-MPS) was prepared by following the steps similar to our previous work.[22] In brief, VBC and γ-MPS (molar ratio: 1 : 1) were reacted at 70 °C for 24 h with 0.8% AIBN as the initiator. The obtained copolymer was purified through toluene dissolution/hexane precipitation and then dissolved in toluene to prepare a solution of 0.49 g mL^{-1} copolymer. The average molecular weight (M_w) of poly(VBC-*co*-γ-MPS) was 22,729 measured by gel permeation chromatography GPC. And the structure of poly(VBC-*co*-γ-MPS) and BPPO are shown in Scheme 1.

Preparation of hybrid membranes

For preparation of hybrid membranes, BPPO was blended with poly(VBC-*co*-γ-MPS) in DMF. Then, the blends were quaternized by TMA before a sol–gel process. The whole process is illuminated in Scheme 2. Detailed preparation procedures are as follows: BPPO and poly(VBC-*co*-γ-MPS) were added in DMF by turn and stirred rapidly at room temperature. After 15 min, the TMA solution was added dropwise and the solution became turbid. Then,
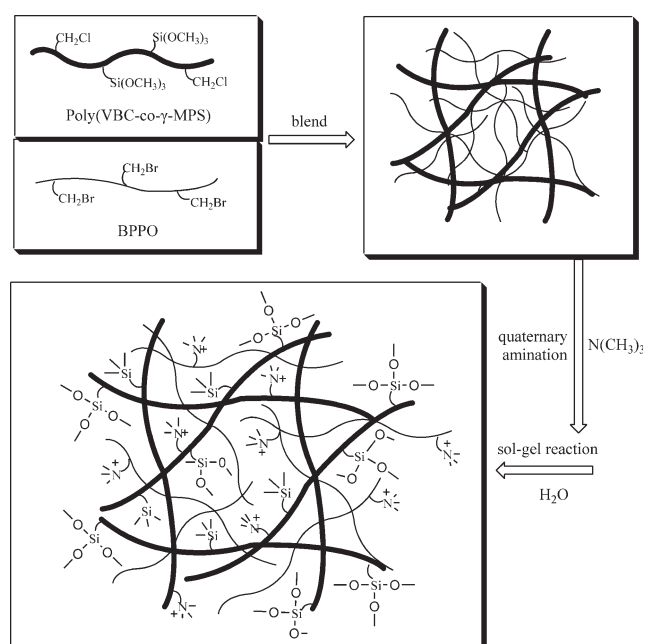
Scheme 2 Synthesis of hybrid membranes by blending BPPO with poly(VBC-*co*-γ-MPS).

ethanol was added until the turbidity gradually disappeared and the solution became transparent. After 30 min of further stirring, deionized water was added dropwise to start the sol–gel reaction.

The sol–gel reaction continued at room temperature for 12 h. Then, the solution was cast onto a Teflon plate for solvent volatilization for 2 days. Subsequently, it was dried in a vacuum oven according to the following procedures: 60–100°C at the rate of 10 °C/h, and 100–130°C at the rate of 10 °C/2h. The hybrid membranes obtained were free-standing without any supporting materials and had a high flexibility and strength.

During membrane preparation, the molar ratio of TMA to the total Br of BPPO and Cl of poly(VBC-co-γ-MPS) was set at 1.5 : 1 while the molar ratio of H_2O to the -$Si(OCH_3)_3$ of poly(VBC-co-γ-MPS) was set at 10 : 1. The mass fraction of BPPO was varied from 40, 45, 53, 63, 71 to 83%. The corresponding membranes were named as membranes A, B, C, D, E, and F.

Characterizations

For analysis of the composition and chemical structure of the hybrid membrane, FTIR was performed by using a Vector 22 Fourier transform infrared spectrometer (Bruker). The thermal properties were investigated by the thermogravimetric analysis (Shimadzu TGA-50H analyzer) under air flow and with a heating rate of 10 °C min^{-1}. An Instron universal tester (Model 1185) was used to measure the tensile properties at 25°C with dumbbell shape specimens at a crosshead speed of 25 mm min^{-1} and with an initial gauge length of 25 mm. The tensile strength (TS) and elongation at break (E_b) values were recorded. The membranes were fractured in liquid nitrogen for cross section morphology observation by scanning electron microscopy (XT30 ESEM-TMP PHILIP).

Water uptake (W_R) was measured to investigate the hydrophilicity of membrane.[22] The sample was dried in vacuum at 80°C until a constant weight m_1 was attained, and the sample was immersed in distilled water for 2 days. Afterwards, the surfaces of the sample were dried and the sample was weighted as m_2. The W_R was calculated according to the following equation: $W_R = (m_2 - m_1)/m_1 \times 100\%$.

The ion-exchange capacity in the Cl^- form (IEC_{Cl}) was measured according to our previous work.[25] The sample was firstly dried to a constant weight and then converted to the Cl^- form by immersing it in $1M$ NaCl. Distilled water was used to wash off the excessive NaCl. Then, the sample was immersed in $0.5M$ Na_2SO_4 for 2 days. The anion-exchange capacity was obtained by determining the amount of the exchanged Cl^- by titration with $0.1M$ $AgNO_3$. The IEC_{Cl} value was calculated from the released

chloride ions and expressed as mmol g^{-1} of dry membrane (in the Cl^- form).

For investigation of chemical stability, the hybrid membranes were treated with $2M$ NaOH for different time (1, 2, 4, and 6 days, respectively).[15] Then, the IEC_{Cl} values were measured. To highlight the difference, the IEC_{Cl} values before the treatment with NaOH was denoted as $IEC_{Cl,0}$ and the values after the treatment as $IEC_{Cl,t}$. The ratio of $IEC_{Cl,t}$ to $IEC_{Cl,0}$ was calculated to determine the alkali resistance.

The hydroxyl conductivity of membrane was measured by using the normal four-point probe technique according to our previous work.[22] Before measurement, the membranes were transformed to the OH^- form in a KOH solution ($0.5M$ for 2.5 h, then $2M$ for 4 h). Then, they were washed to remove the absorbed alkaline. The measuring cell (Teflon) consisted of two stainless steel flat outer current-carrying electrodes (2 cm apart) and two platinum wire inner potential-sensing electrodes (1 cm apart). A membrane sample (1 cm ×4 cm) was fully hydrated and mounted on the cell. The impedance was recorded using an Auto lab PGSTAT 302 (Eco Chemie, Netherlands) (galvanostatic mode; ac current amplitude, 0.1 mA; frequency, 1 MHz to 50 Hz).

The hydroxyl conductivity (κ) was calculated according to the following equation:

$$\kappa = \frac{L}{RWd}$$

where R is the membrane resistance, L is the distance between potential-sensing electrodes, and W and d are the width and thickness of the membrane, respectively.

The molecular weight was determined on a Waters 150C GPC equipped with three Ultrastyragel columns (500, 103, 104 Å) in series and RI 2414 detector, and tetrahydrofuran (THF) was used as eluent at a flow rate of 1.0 mL min^{-1}. Monodisperse polystyrene was used to calibrate molecular weight.

RESULTS AND DISCUSSION

FTIR spectra

Figure 1 shows the FTIR spectra of the hybrid membranes. All the spectra contain a large band between 3100 and 3700 cm^{-1}, which is ascribed to the stretching vibration of OH groups from residual water and Si—OH groups of poly(VBC-co-γ-MPS).[22] The other bands or peaks are corresponding to the following vibrations:

- The bands between ∼ 2850 and ∼ 3030 cm^{-1}—the stretching vibrations of CH_3, CH_2, and CH groups (ν and δ)[20];
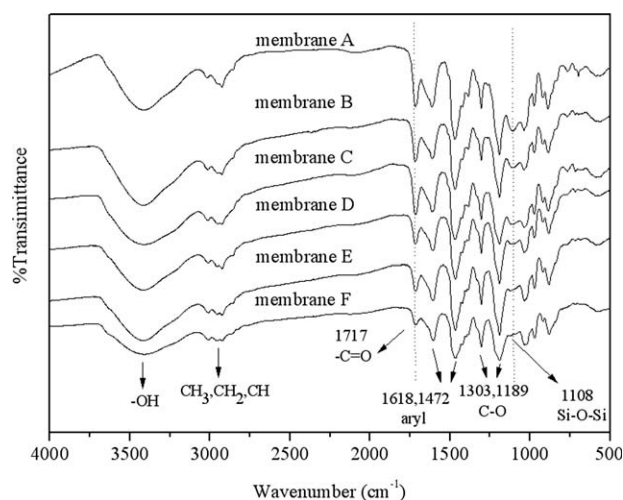- The bands at ∼ 1615 cm^{-1} and ∼ 1475 cm^{-1}—the vibrations of phenyl groups[26];

Figure 1 FTIR spectra of the hybrid membranes.

- The band at ~ 1715 cm^{-1}—the stretching vibration of carbonyl in ester;
- The peaks at ~ 1300 and ~ 1190 cm^{-1}—the symmetric and asymmetric stretching vibrations of C—O—C.[20]
- The peak at ~ 1110 cm^{-1}—the stretching vibration of Si—O—Si.[20]

During the preparation of the hybrid membranes, the dosage of poly(VBC-*co*-γ-MPS) decreased from membrane A to membrane F. Accordingly, the contents of Si and C=O groups (both from poly(VBC-*co*-γ-MPS)) should decrease. This can be proved by the gradual decrease in the intensity of absorption band at ~ 1715 cm^{-1} ($\nu_{C=O}$) and ~ 1110 cm^{-1} (Si—O—Si) [Fig. 1(a–f)].

Morphology

The morphology of membrane is very important and observed by the SEM measurement commonly. In this article, membrane A, B, and E are chosen for SEM observations and their SEM images are shown in Figure 2(a–c). For comparison, the SEM image of the membrane prepared from only BPPO is presented in Figure 2(d).

As compared with some other BPPO-based blend membranes[23] and hybrid membranes,[27] the morphology of hybrid membranes here is superior. This suggests that the miscibility between BPPO and poly(VBC-*co*-γ-MPS) is generally excellent.

The SEM images of membranes are different from each other, and the result can demonstrate the homogeneity of membranes with different mass fraction ratio of BPPO. In the case of membrane A [Fig. 2(a)], there are some aggregations (4–14 μm in diameter) on the fractured surface, which are caused by the phase separation between BPPO and
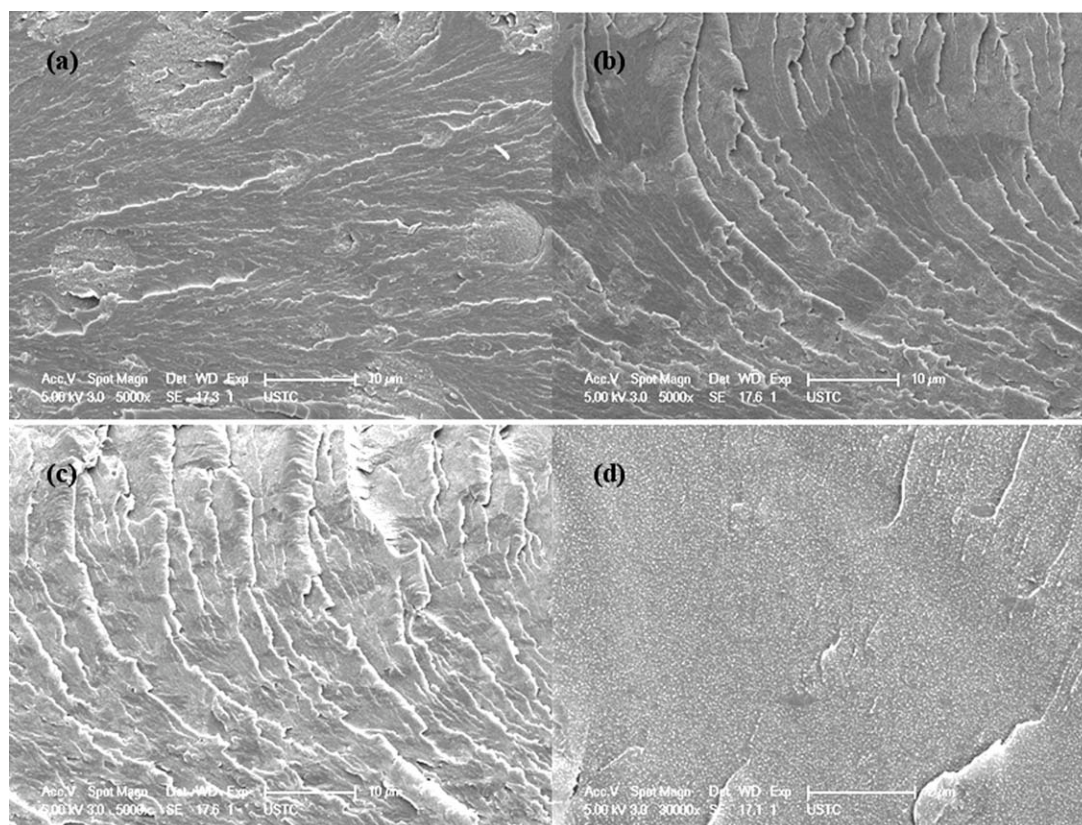

Figure 2 SEM images of (a) membrane A, (b) membrane B, (c) membrane E, and (d) pure BPPO membrane.

TABLE I
Properties of the Hybrid Membranes

Membrane	A	B	C	D	E	F
W_R (%)	51.8	49.7	46.4	43.2	41.7	32.4
IEC_{Cl} (mmol g^{-1})	2.19	2.24	2.21	2.22	2.27	2.25
IDT (°C)[a]	215.9	223.5	228.5	210.8	214.8	225.1
T_d (°C)[b]	248.4	260.7	258.9	242.7	247.6	252.9
TS (MPa)	32.4	29.9	34.2	31.3	31.7	29.2
E_b (%)	8.6	7.7	7.8	9.8	11.1	10.6

[a] IDT is the initial decomposition temperature determined from TGA thermograms.

[b] The thermal degradation temperatures (T_d) are defined as the temperature at which the weight loss reaches 5 wt % in TGA thermograms.

poly(VBC-*co*-γ-MPS). When the content of BPPO increases slightly, the aggregations disappear and some centralized dark domains appear on the fracture surface of membrane B [Fig. 2(b)], similar phenomena was also observed in our previous research,[23] the result shows that the phase separation between BPPO and poly(VBC-*co*-γ-MPS) is reduced and the miscibility of BPPO and poly(VBC-*co*-γ-MPS) is enhanced. With a further increase in the content of BPPO from membrane E [Fig. 2(c)] to pure BPPO membrane [Fig. 2(d)], the centralized dark domains are dispersed and finally disappear, and the fracture surfaces of membrane become uniform, indicating the enhancement of compatibility.

Ion exchange capacity

The IEC values of the hybrid membranes in the Cl$^-$ form (IEC_{Cl}) are presented in Table I. The values are in the range of 2.19–2.27 mmol g^{-1}, which are higher than those of our previous membranes (1.74–2.17 mmol g^{-1}), which were prepared from poly(VBC-*co*-γ-MPS) and monophenyltriethoxysilane (EPh).[22] It should be noted that the theoretical IEC value of BPPO (2.32 mmol g^{-1}) is higher than poly(VBC-*co*-γ-MPS) (2.17 mmol g^{-1}) and EPh in the previous membrane cannot be charged, therefore the addition of EPh and BPPO will decrease and increase the IECs of membranes, respectively. It is the reason why IEC values of the hybrid membranes are higher than the previous hybrid membranes.

Note that there is no significant increase in the IEC values for membranes A to membrane F even though they have different compositions. This is mainly because BPPO has an IEC_{Cl} value (2.32 mmol g^{-1}) close to that of poly(VBC-*co*-γ-MPS) (2.17 mmol g^{-1}).[22] Therefore, the charge density of the hybrid membrane does not vary much even though membranes A to F have different mass ratios of BPPO to poly(VBC-*co*-γ-MPS).

Water uptake (W_R)

As shown in Table I, the hybrid membranes have a water uptake (W_R) of 32.4–51.8%, and this is similar

to those of some reported anion-exchange membranes (48.2–54.4%) for fuel cell application.[28,29] When it comes to our previous membranes based on only poly(VBC-*co*-γ-MPS), their W_R values were in the range of 16–35%.[22] In comparison, there is an increase in W_R for the hybrid membranes. This suggests that the membrane hydrophilicity is enhanced and favorable for fuel cell applications.

The W_R value of pure BPPO membrane is 31.1%, and this value is lower than those of the hybrid membranes. Hence, BPPO component alone is not the main cause for the increase in W_R of hybrid membranes. Rather, the change in the membrane structure plays the vital role. As evidenced by SEM images (section "Morphology"), the hybrid membranes have phase separation at a high poly(VBC-*co*-γ-MPS) content. Accordingly, the membrane structure becomes loose and favorable for water absorption in the membrane matrix. Naturally, as BPPO content increases from membrane A to F, phase separation diminishes gradually and the W_R values follow a general decreasing trend in Table I. It should be noted that the loose structure caused by phase separation may lead to a high fuel crossover. However, for the hybrid membranes, the presence of crosslinked silica network (Si—O—Si) formed during the sol–gel reaction may reduce the channel allowing the passage of methanol molecules, so that the resistance to the diffusion of methanol is increased.[17,30] As well known, for anion exchange membrane used in direct methanol fuel cells (DMFCs), the ion transport within the membrane in an operating alkaline membrane direct methanol fuel cells (AMDMFCs) will be from the cathode to the anode and water will actually be electro-osmotically transported from cathode to anode too, while the direction of methanol crossover within the membrane will be from anode to cathode.[2] So the methanol permeability will be reduced markedly for the opposing transport direction furthermore. In general, the hybrid membranes would not suffer fuel permeation seriously.

Chemical resistance

For application in fuel cells, chemical stability, especially the alkali resistance of membrane, is important. According to previous research, the chemical stability of membrane can be evaluated by the change in the IEC of the membrane under different conditions (in hot water[31] or in an alkali solution[15,32]). Here, 2M NaOH was used. Membranes B, C, D, and E were chosen for measurement. For each membrane, the original IEC values ($IEC_{Cl,0}$) and the IEC values after immersion in NaOH for different time ($IEC_{Cl,t}$) were recorded. The ratios of $IEC_{Cl,t}$ to $IEC_{Cl,0}$ (IEC ratio) were calculated and illustrated in Figure 3.

As time elapses, the IEC ratio of each hybrid membrane initially decreases sharply and afterwards
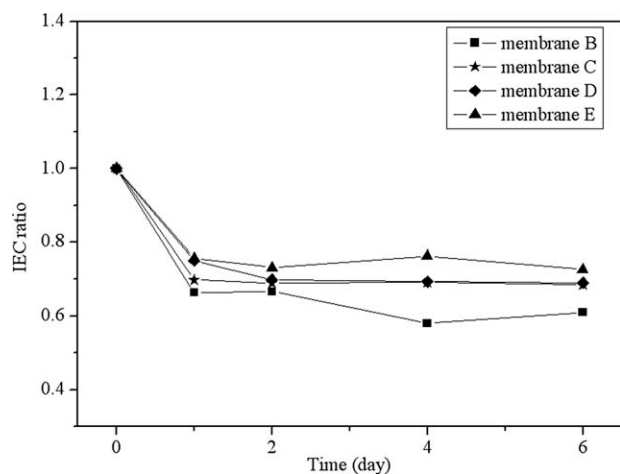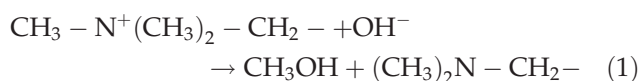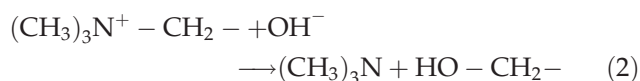
Figure 3 Alkaline resistances and the ratios of $IEC_{Cl,t}$/ $IEC_{Cl,0}$, as a function of the exposure time in 2 mol L^{-1} NaOH at 25°C.

levels off. This phenomenon has been observed in our previous research.[15] The hybrid membranes have functional groups such as ester, siloxane, and quaternary ammonium groups, and these groups are all electrophilic and subject to hydrolysis in alkaline. Nevertheless, a dual network is constructed by polymer chains and silica after the sol–gel and heat treatment of poly(VBC-*co*-γ-MPS). Hence, the decomposition of ester or siloxane groups from poly(VBC-*co*-γ-MPS) should be less serious. The loss of IEC is mainly due to the decomposition of the quaternary ammonium groups according to the following mechanisms[2]:

$$CH_3 - N^+(CH_3)_2 - CH_2 - +OH^-$$
$$\rightarrow CH_3OH + (CH_3)_2N - CH_2 - \quad (1)$$

and

$$(CH_3)_3N^+ - CH_2 - +OH^-$$
$$\longrightarrow (CH_3)_3N + HO - CH_2 - \quad (2)$$

After the decomposition of these groups, the IECs remain in the range of 60–75% of the original IEC values ($IEC_{Cl,0}$). These residual IEC values are much higher than those reported in our previous work (35–62%).[32] This suggests that the short-term chemical stability of the hybrid membranes is acceptable for evaluation of their fuel cell performances.

Among the four hybrid membranes, membrane B has the lowest BPPO content and IEC ratio. This mainly results from the poorer miscibility of the two polymer components in the membrane, as shown in the SEM image in section "Morphology." Naturally, as BPPO content increases, the miscibility is enhanced. Hence, the chemical stability increases, leading to a gradual increase in the IEC ratio from membrane B to membrane E (Fig. 5).

Thermal stability (TGA analysis)

Thermal stability is an important indicator for membrane performances in fuel cells. The TGA and DrTGA diagrams of hybrid membranes are illustrated in Figure 4.

As shown in the TGA diagrams, all samples lose weight slightly before 80°C and there is no obvious loss of weight from 80 to 230°C. Since the initial weight loss before 80°C is caused by the loss of absorbed water and residual solvent, it will be not considered in the following discussion.

Table I lists the initial decomposition temperatures (IDT) and thermal degradation temperatures (T_d: defined as the temperature at 5% weight loss). The IDT values are in the range of 226–234°C while the T_d values are in the range of 248–259°C. As
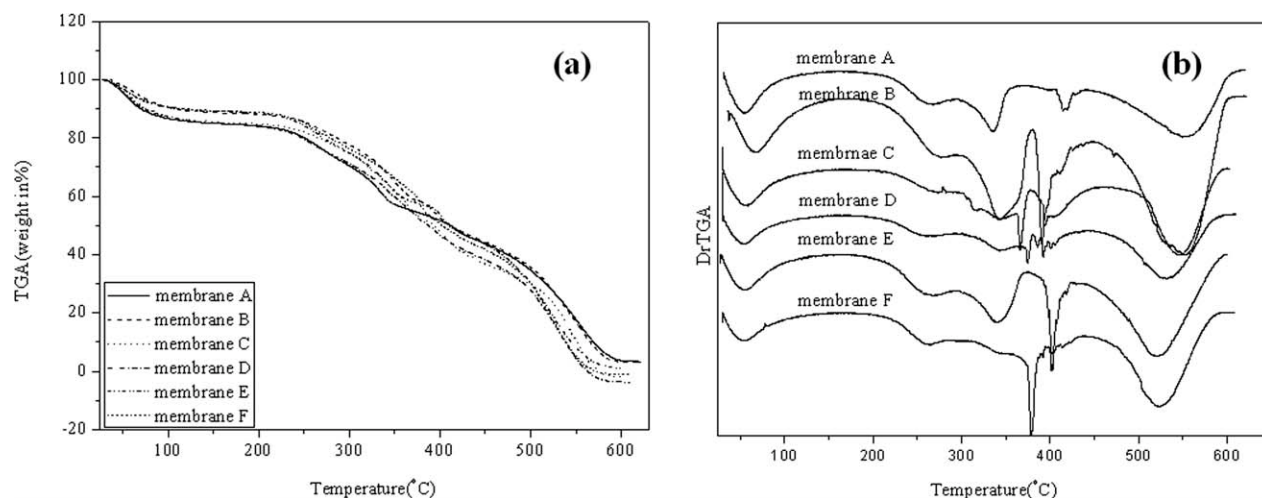

Figure 4 TGA (a) and DrTGA (b) diagrams of hybrid membranes at a heating rate of 10 °C min^{-1} under air flow.
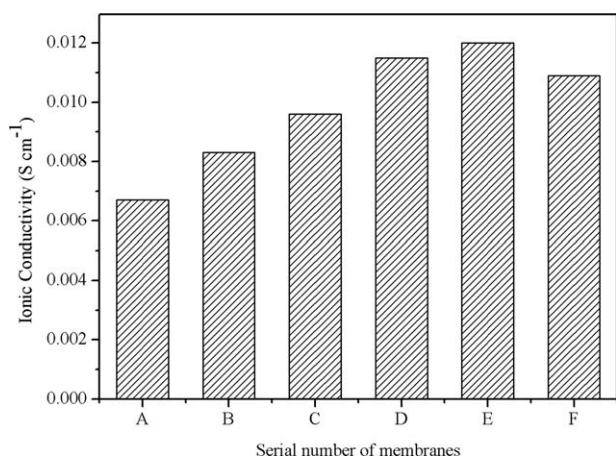
Figure 5 Conductivities of the hybrid membranes in the OH⁻ form.

compared with other reported hybrid membranes for AMFC applications, these hybrid membranes have superior thermal stabilities[28] and thus are promising for use in fuel cells at higher temperatures. Notably, the IDT values of the hybrid membranes (226–234°C) are close to those of our previous membranes prepared from only poly(VBC-co-γ-MPS) (IDT: 238–260°C),[22] but the T_d values (248–259°C) are lower than those in our previous research (257–300°C). The slight decline of thermal stability results from the incompatibility between two polymer components or between inorganic and organic components (see section "Morphology").

DrTGA diagrams [Fig. 4(b)] give more details about the thermal decomposition. Obviously, all the membranes have five peaks. At the low temperature (30–120°C), the primary weight loss is caused by the evaporation of residual solvent and water. The second weight loss of the membrane in the range of 210–290°C is due to the decomposition of quaternary ammonium groups.[22,25] The third loss in the range of 320–345°C is due to the decomposition of the ester groups of poly(VBC-co-γ-MPS).[22] The fourth loss in the range of 360–420°C and the last loss in the range of 465–590°C are attributed to the decomposition of the carbon chain[23] and phenyl groups,[22] respectively.

Tensile properties

In our previous work,[22] PETEX woven screening fibers were used as the supporting material for poly(VBC-co-γ-MPS) membranes because the hybrid membrane layer was too brittle. Here, the supporting material is not necessary since the membrane's flexibility is enhanced after blending with BPPO. As shown in Table I, the TS (tensile strength) and E_b (the elongation at break) values of the hybrid mem-

branes are in the range of 29.2–34.2 MPa and 7.7–11.1%, respectively. These properties are acceptable as compared with other reported membranes.[29,33]

For different membranes, the TS values are similar, suggesting that these hybrid membranes have close mechanical strength. On the other hand, the E_b values follow a general increasing trend as BPPO content increases. It is an abnormal phenomena as there are abundant alkyl chains (-CH$_2$-CH-)$_n$ in the poly(VBC-co-γ-MPS) and the alkyl chains are usually considered to be more flexible than poly phenyl backbones. However, there are abundant crosslinked silica networks (-Si—O—Si-) which were formed during the sol–gel reaction of poly(VBC-co-γ-MPS). Because of the brittleness of the crosslinked silica networks, poly(VBC-co-γ-MPS) will be less flexible than BPPO. So the increase of the content of BPPO will increase the flexibility of the membranes. An enhancement of membrane homogeneity at higher BPPO content can also contribute to the higher flexibility of the membrane.

Membrane conductivity

The hydroxyl conductivity values of hybrid membranes, as shown in Figure 5, are in the range of 0.0067–0.012 S cm⁻¹. Those values are comparable to the reported fluoropolymer-based membranes[33] but higher than some other anion-exchange membranes prepared from nonfluorinated polymers.[15]

As BPPO content increases from membrane A to membrane F, the conductivity generally increases from 0.0067 S cm⁻¹ to 0.012 S cm⁻¹. For the membrane with higher BPPO content, the increasing trend slows down. Membranes D–F have similar values and their conductivities are in the range of 0.011–0.012 S cm⁻¹.

In our previous work, the hybrid membrane prepared from poly(VBC-co-γ-MPS) had a low ion conductivity (2.27×10^{-4} to 4.33×10^{-4} S cm⁻¹).[22] In comparison, the hybrid membranes here have much higher ion conductivities, and this is contributed by many factors. Firstly, no woven fiber supporting materials are used for the hybrid membranes, so there are more ion conducting channels formed by packing sufficient conductive hybrid gels.[34] Secondly, the improved hydrophilicity of membrane results in a significant increase in ion conductance. Thirdly, after blending with BPPO, the membrane can have loose Si—O—Si networks in the matrix. To date, the influence of silica component on membrane conductivity has been extensively investigated but there is no agreement. Generally, there are two opposite effects. On one hand, the unreacted —SiOH from silica has a strong bonding ability with H$_2$O molecules and is in favor of water retention and promotion of ion transfer.[35] Hence, proper silica content

is favorable for ion conduction, and this has been confirmed by our previous work.[36] On the other hand, excessive inorganic Si—O—Si network may retard the mobility of the membrane chain and thus restrict the formation of ionic cluster regions and channels.[37] Here the latter effect may play the main role.

Another factor that can influence the hydroxyl (OH⁻) conductivity is the formation of bicarbonate and carbonate. In our previous work,[15,22] the membrane samples (in the OH⁻ form) were exposed to air for some time before conductivity measurement. The CO_2 in the air would lead to the carbonation of the samples[38] and is unfavorable for ion conduction.[39] However, the carbonation of the alkali anion-exchange membrane (AAEM) is a common problem during the operation of direct methanol fuel cells.[39] Therefore, the conductivity values of partially carbonated membranes here are also valuable.

Among the hybrid membranes, membranes D and E (BPPO content in the range of 60–75%) demonstrate the highest ion conductivities. Besides, their other physicochemical properties (such as hydrophilicity and homogeneity) are proper and qualified for use in fuel cells. Hence, the membranes with 60–75 wt % BPPO are recommended for application in fuel cells.

CONCLUSIONS

A series of hybrid anion-exchange membranes were prepared by blending BPPO with poly(VBC-*co*-γ-MPS). As compared with the membranes prepared from pure poly(VBC-*co*-γ-MPS),[22] these hybrid membranes exhibited remarkably improved flexibility and excellent membrane-forming property. The other properties, such as water uptake (W_R), ion exchange capacity (IEC), mechanical strength, thermal stability, and alkali resistance, were enhanced or maintained. Especially, the OH⁻ conductivity significantly increased from 2.27–4.43×10^{-4} S cm⁻¹ to 0.6–1.2×10^{-2} S cm⁻¹. These results indicate the success in modifying the membrane by blending with BPPO.

Among these hybrid membranes, the membranes with 60–75% BPPO exhibited the best performances: IEC in the range of 2.20–2.25 mmol g⁻¹, W_R in the range of 40–50%, OH⁻ conductivity as high as 0.0115–0.012 S cm⁻¹, and good thermal and physicochemical stability. Hence, they are promising for use in AMFCs even though the single cell performance is not evaluated due to our experimental limitations.

References

1. Smitha, B.; Sridhar, S.; Khan, A. A. J Membr Sci 2005, 259, 10.
2. Varcoe, J. R.; Slade, R. C. T. Fuel Cells 2005, 5, 187.
3. Ong, A. L.; Bottino, A.; Capannelli, G.; Comite, A. J Power Sources 2008, 183, 62.
4. Lehtinen, T.; Sundholm, G.; Holmberg, S.; Sundholm, F.; Björnbom, P.; Bursell, M. Electrochim Acta 1998, 43, 1881.
5. Kumar, G. G.; Kim, P.; Nahm, K. S.; Elizabeth, R. N. J Membr Sci 2007, 303, 126.
6. Lufrano, F.; Baglio, V.; Staiti, P.; Arico, A. S.; Antonucci, V. J Power Sources 2008, 179, 34.
7. Karlsson, L. E.; Jannasch, P. J Membr Sci 2004, 230, 61.
8. Carbone, A.; Pedicini, R.; Portale, G.; Longo, A.; D'Ilario, L.; Passalacqua, E. J Power Sources 2006, 163, 18.
9. Zhang, H.; Fan, X.; Zhang, J.; Zhou, Z. Solid State Ionics 2008, 179, 1409.
10. Rikukawa, M.; Sanui, K. Prog Polym Sci 2000, 25, 1463.
11. Cruickshank, J.; Scott, K. J Power Sources 1998, 70, 40.
12. Roziere, J.; Jones, D. J. Annu Rev Mater Res 2003, 33, 503.
13. Zhang, Y.; Zhang, H.; Zhai, Y.; Zhu, X.; Bi, C. J Power Sources 2007, 168, 323.
14. Jung, D. H.; Cho, S. Y.; Peck, D. H.; Shin, D. R.; Kim, J. S. J Power Sources 2002, 106, 173.
15. Wu, Y.; Wu, C.; Xu, T.; Lin, X.; Fu, Y. J Membr Sci 2009, 338, 51.
16. Niepceron, F.; Lafitte, B.; Galiano, H.; Bigarr, J.; Nicol, E.; Tassin, J. F. J Membr Sci 2009, 338, 100.
17. Xiong, Y.; Liu, Q. L.; Zhu, A. M.; Huang, S. M.; Zeng, Q. H. J Power Sources 2009, 186, 328.
18. Uragami, T.; Okazaki, K.; Matsugi, H.; Miyata, T. Macromolecules 2002, 35, 9156.
19. Teng, X. G.; Zhao, Y. T.; Xi, J. Y.; Wu, Z. H.; Qiu, X. P.; Chen, L. Q. J Power Sources 2009, 189, 1240.
20. Wu, Y. H.; Wu, C. M.; Gong, M.; Xu, T. W. J Appl Polym Sci 2006, 102, 3580.
21. Wu, Y. H.; Wu, C. M.; Xu, T. W.; Fu, Y. X. J Membr Sci 2009, 329, 236.
22. Wu, Y. H.; Wu, C. M.; Xu, T. W.; Yu, F.; Fu, Y. X. J Membr Sci 2008, 321, 299.
23. Wu, L.; Xu, T. W.; Wu, D.; Zheng, X. J Membr Sci 2008, 310, 577.
24. Xu, T. W.; Wu, D.; Wu, L. Prog Polym Sci 2008, 33, 894.
25. Wu, C. M.; Xu, T. W.; Yang, W. H. Eur Polym Mater 1901 2005, 41.
26. Li, Y.; Xu, T. W.; Gong, M. J Membr Sci 2006, 279, 200.
27. Ma, Z. G.; Gao, J. D.; Huai, Y. J.; Guo, J.; Deng, Z. H.; Suo, J. S. J Sol–Gel Sci Technol 2008, 48, 267.
28. Danks, T. N.; Slade, R. C. T.; Varcoe, J. R. J Mater Chem 2002, 12, 3371.
29. Herman, H.; Slade, R. C. T.; Varcoe, J. R. J Membr Sci 2003, 218, 147.
30. Fei, S.-T.; Wood, R. M.; Lee, D. K.; Stone, D. A.; Chang, H.-L.; Allcock, H. R. J Membr Sci 2008, 320, 206.
31. Danks, T. N.; Slade, R. C. T.; Varcoe, J. R. J Mater Chem 2003, 13, 712.
32. Wu, C. M.; Wu, Y. H.; Xu, T. W.; Fu, Y. X. J Appl Polym Sci 2008, 107, 1865.
33. Slade, R. C. T.; Varcoe, J. R. Solid State Ionics 2005, 176, 585.
34. Tezuka, T.; Tadanaga, K.; Matsuda, A.; Hayashi, A.; Tatsumisago, M. Electrochem Commun 2005, 7, 245.
35. Miyake, N.; Wainright, J. S.; Savinell, R. F. J. Electrochem Soc 2001, 148, A905.
36. Wu, Y. H; Wu, C. M.; Varcoe, J. R.; Poynton, S. D.; Xu, T. W.; Fu, Y. X. J Power Sources, 195, 3069.
37. Kim, D. S.; Park, H. B.; Rhim, J. W.; Lee, Y. M. Solid State Ionics 2005, 176, 117.
38. Theodorou, V.; Skobridis, K.; Tzakos, A. G.; Ragoussis, V. Tetrahedron Lett 2007, 48, 8230.
39. Varcoe, J. R.; Slade, R. C. T.; Lam How Yee, E.; Poynton, S. D.; Driscoll, D. J.; Apperley, D. C. Chem Mater 2007, 19, 2686.